Biosensors and Bioelectronics 131 (2019) 171–177

Contents lists available at ScienceDirect

Biosensors and Bioelectronics

journal homepage: www.elsevier.com/locate/bios

Development of an electrochemical impedimetric immunosensor for Corticotropin Releasing Hormone (CRH) using half-antibody fragments as elements of biorecognition

B.G. Duran[a,c], E. Castañeda[b], F. Armijo[b,c,*]

[a] Instituto de Física Pontificia Universidad Católica de Chile, Av. Vicuña Mackenna 4860, 7820436 Macul, Santiago, Chile
[b] Facultad de Química y de Farmacia, Departamento de Química Inorgánica, Laboratorio de Bioelectroquímica, Pontificia Universidad Católica de Chile, Av. Vicuña Mackenna 4860, 7820436 Macul, Santiago, Chile
[c] Centro de Investigación en Nanotecnología y Materiales Avanzados CIEN-UC Pontificia Universidad Católica de Chile, Av. Vicuña Mackenna 4860, 7820436 Macul, Santiago, Chile

ARTICLE INFO

Keywords:
Electrochemical
Immunosensor
Gold nanoparticles
Corticotropin Releasing Hormone
Stress

ABSTRACT

An electrochemical impedimetric immunosensor was developed for the detection of the neuropeptide Corticotropin Releasing Hormone (CRH) based on the immobilization of half-antibody fragments on gold nanoparticles (AuNp). Then, the optimal conditions for the obtainment of AuNp through electroplating on a bare gold electrode were studied. The results showed that the obtainment of AuNp at a fixed potential of −0.2 V for 330 s, at 80 °C and $2{\cdot}10^{-3}$ mol·L^{-1} of $HAuCl_4$ generates an adequate nanostructured surface and is a highly reproducible method. Also, the optimal conditions for immobilizing the half-antibody on AuNp were studied. The interaction of the CRH with the recognition layer of the immobilized half-antibody on the nanostructured surface was carried out by incubation at 4 °C for 2 h. A dissolution of $[Fe(CN)_6]^{4-}/[Fe(CN)_6]^{3-}$ as a redox probe was used to study the electrochemical responses of the nanostructured surface and the immobilization processes of the half-antibody and detection of CRH, using cyclic voltammetry and electrochemical impedance spectroscopy. An immunosensor was obtained for the specific detection of CRH, within a range of 10.0–80.0 μg mL^{-1}, with a limit of detection of 2.7 μg mL^{-1} and a limit of quantification of 9.2 μg mL^{-1}. Additionally, the association constant between the CRH and the immobilized half-antibody was calculated at $1.96{\cdot}10^{5}$ M^{-1}.

1. Introduction

The peptide family of the Corticotropin-releasing hormone (CRH) and its receptors are possibly the most essential stress response components in vertebrate organisms (Endsin et al., 2017). For this reason, there is a motivation to study the physiopathology of psychiatric disorders in order to identify biological markers that can be modulated to prevent or treat disease. Given that the hypothalamic-pituitary-adrenal axis is the main hormone mediator for the stress response, this system and its function have been a primordial objective of exploring the physiopathology of post-traumatic stress disorder (Dunlop and Wong, 2019). One of these biological markers for studying stress is CRH, which is a 41-amino acid peptide hormone of approximately 4.7 kDa (Knoop et al., 2017). Several studies have determined that CRH is in the ng·mL^{-1} range in blood (Glynn et al., 2007; Knoop et al., 2017; Sandman et al., 2006; Strong et al., 2006). The determination of CRH has been performed indirectly through the quantification of the mRNA expression of CRH and/or the peptide through immunohistochemistry (Santibañez et al., 2005, 2006). Additionally, the use of techniques such as radioimmunoassays (RIA) and Enzyme-Linked Immunosorbent Assay (ELISA) has allowed for the evaluation of temporary changes in the extracellular CRH (Merali et al., 2004).

The first immunoassay method reported for estimating CRH and cortisol was described by Cook (2001). This method describes the measurement of cortisol or CRH directly from the brain, through a microdialysis probe using an antibody-linked assay. These antibodies are affixed on a platinum electrode within the probe. Determination of bound CRH or cortisol is performed via an indirect assessment of competitive ligand also binding, and conjugated to horseradish peroxidase (HRP) (Cook, 2001).

While immunoassays are effectively using laboratory techniques that are primarily based on the optic principle, they require the

* Corresponding author at: Facultad de Química y de Farmacia, Departamento de Química Inorgánica, Laboratorio de Bioelectroquímica, Pontificia Universidad Católica de Chile, Av. Vicuña Mackenna 4860, 7820436 Macul, Santiago, Chile.
E-mail address: jarmijom@uc.cl (F. Armijo).

https://doi.org/10.1016/j.bios.2019.02.017
Received 20 December 2018; Received in revised form 5 February 2019; Accepted 12 February 2019
Available online 19 February 2019
0956-5663/

enrichment and purification of the sample before analysis. Also, are expensive and slow.

Therefore, strategies have been recently proposed for the amplification of the signal using different nanostructured materials in order to increase the sensitivity of these optical and electrochemical devices (Pang et al., 2018; Ren et al., 2017a, 2017b, 2017c, 2018; Yang et al., 2017a, 2017b). Among the advantages of these devices is their ability to use diverse recognition elements, like enzymes, antibodies, nucleic acids, and whole cells, and recent recognition elements, such as phages, aptamers and affibodies (Justino et al., 2015). Also, there is a possibility to develop low cost and large-scale production microelectrodes that can useful for multiplexing, and, at the same time, be highly suitable for being used in very small sample volumes (microliters to nanoliters). Finally, the minimum of electrochemical interference elements in real samples makes electrochemical methods the most suitable to be used in complex samples. Therefore the research, development, optimization and characterization of new electrochemical immunosensor is of vital importance (Ricci et al., 2012).

On the other hand, there are currently no impedimetric immunosensors described in literature for the detection of CRH. Then, the development of the use of electrochemical immunosensors, due to their excellent analytical capacities, as well as their sensitivity, reproducibility, simplicity of construction and feasible miniaturization, would lead it to be considered a promising alternative to monitor elevated levels of cortisol or CRH (Moreno-Guzmán et al., 2010; Kaushik et al., 2013; Moreno-Guzman et al., 2012a, 2012b; Yamaguchi et al., 2013; Zhou et al., 2004). Also, the CRH hormone is classified as a prohibited substance by the World Anti-Doping Agency (WADA), thus requiring a method for detecting CRH in the bloodstream (serum and plasma) (Knoop et al., 2017).

On the other hand, the orientation of the antibody when immobilized on a surface is essential for manufacturing the immunosensor. The simple physical adsorption of these may result in a loss of sensitivity and reproducibility (Makaraviciute and Ramanaviciene, 2013; Ricci et al., 2012). Additionally, a large number of covalent antibody immobilizations have been performed using glutaraldehyde, carbodiimide, succinimide, biotin, etc. (Hermanson, 2013). This covalent bond produces, in addition to physical adsorption, a random orientation that may result in reduced sensitivity due to the fact that the antigen-antibody interaction only occurs in the variable region of the antibody (Hermanson, 2013).

Moreover, it has been demonstrated that biomolecules, such as antibodies, conserve their activity when immobilized at nanoparticle-modified surfaces, as they provide a good biocompatibility (Jazayeri et al., 2016). Also, the ease of preparation of gold nanoparticles (AuNp) on different electrode surfaces using electrochemical methods makes them suitable for the development of modified electrodes (Liu et al., 2005; Park et al., 2011; Saldan et al., 2018; Xiao et al., 2016). Other characteristics of AuNp include their high ratio of surface area to volume, high surface energy and function as an electron carrier between biomolecules and the electrode surface. Furthermore, the use of AuNp allows the immunosensor to show a high level of stability in comparison to physical adsorption on electrode surfaces (Rusling et al., 2009) and also helps to amplify the transfer of electrons (Khan et al., 2013). One of the ways to modify gold nanostructured surfaces is based on the affinity between this thiols and gold to form S-Au bonds or the affinity of gold to form amines and NH-Au bonds, which offers a simple, fast and versatile approach for preparing modified electrodes with low AuNp background capacitance (Liu et al., 2004; Saha et al., 2012; Zhao et al., 2013).

Finally, this study proposes an electrochemical immunosensor using half-antibody fragments (H-Ab) as a molecule receptor medium. H-Ab contains thiol groups which are then covalently immobilized and oriented on the AuNp surface. This has been already studied, and a low loss of the antibody biological activity has been observed (Crivianu-Gaita and Thompson, 2015; Karyakin et al., 2000; Sharma and Mutharasan, 2013; Shen et al., 2017; Wu et al., 2014). This immobilization approach allows for a one-step reaction and simplifies receptor molecule antigen (CRH) immobilization in the preparation of electrochemical immunosensors.

2. Experimental

2.1. Reagents

All reagents were of analytical grade and were used without any previous purification processes. Tetrachloroauric acid trihydrate ($HAuCl_4{\cdot}3H_2O$), KNO_3 and sulfuric acid (H_2SO_4) were purchased from Merck. Potassium ferrocyanide, potassium ferricyanide, sodium citrate, bovine serum albumine (BSA), human serum and other chemicals were purchased from Sigma-Aldrich. PBS (phosphate buffer saline) of pH 7.4 containing 0.1 mol L^{-1} sodium chloride (NaCl, Merck), $2.6{\cdot}10^{-3}$ mol·L^{-1} potassium chloride (KCl, Merck), 0.04 mol L^{-1} potassium hydrogen phosphate (K_2HPO_4, Merck) and 0.01 mol L^{-1} potassium dihydrogen phosphate (KH_2PO_4, Merck) were used as stock solution. Polyclonal antibody produced in rat Anti-CRH, Corticotropin releasing hormone peptide (CRH, 4.757 kDa), and Urocortine I (UCN I) were purchased from Abcam, and all were used as received. All the solutions were prepared using Milli-Q grade water (18 MΩ cm^{-1}).

2.2. Instruments

All electrochemical measurements were performed with a bipotentiostat CHI Instrument 750D with a conventional three electrode system. A Ag/AgCl (1.0 mol L^{-1} KCl) electrode and platinum wire electrode were used as the reference and auxiliary electrode, respectively. A gold disk electrode (0.0314 cm^2, Chi101) was used as working electrode. Complementarily, the morphological structure of gold nanoparticles was analyzed using an LEO 1420 VP emission scanning electron microscope (SEM). The electron micrographs were recorded in a high vacuum mode under an acceleration voltage of 30 kV. All the chemicals and equipment for the electrophoresis analysis of proteins were purchased from Bio-Rad Laboratories Inc.

2.3. Immobilization of gold nanoparticles on gold electrode

Polycrystalline Au electrode was first polished with alumina slurries of 0.05 μm. Then, the electrode was sonicated in ultrapure water for 5 min and thoroughly washed with ultrapure water and ethanol. Afterward, the electrode was immersed in a fresh piranha solution (3:1, H_2SO_4 / H_2O_2) for 30 s, then washed thoroughly with milli-Q water, and subsequently sonicated in ethanol for 4 min and dried. Finally, the Au electrode underwent electrochemical cleaning by scanning the potential between 0.0 and 1.5 V vs. Ag/AgCl (1.0 mol L^{-1} KCl) at 50 mV s^{-1} in 0.5 mol L^{-1} sulfuric acid until the typical voltammetric characteristics of a bare gold electrode were obtained. In order to obtain a reproducible electrodeposition protocol of gold nanoparticles, the pre-treated electrodes were dipped into solution of $HAuCl_4{\cdot}3H_2O$ containing KNO_3 0.1 mol L^{-1} as supporting electrolyte. For this purpose, potential (between -0.1 and −0.5 V), $HAuCl_4$ concentration (1–5 mmol L^{-1}) and temperature (15–80 °C) were studied to obtain the Au/AuNp electrode. These experiments were carried out under the atmosphere of nitrogen.

2.4. Antibody modification electrode

After obtaining a nanostructured surface, we proceeded to study the modification with a biorecognition element (antibody). For this purpose, 2 ways of adsorbing the antibody on the AuNp were studied: A) adsorption of the intact antibody and B) absorption of the antibody by its reduced thiol groups located in the hinge region (half antibody). Intact antibody solution of 1 mg mL^{-1} was stored at −20 °C and

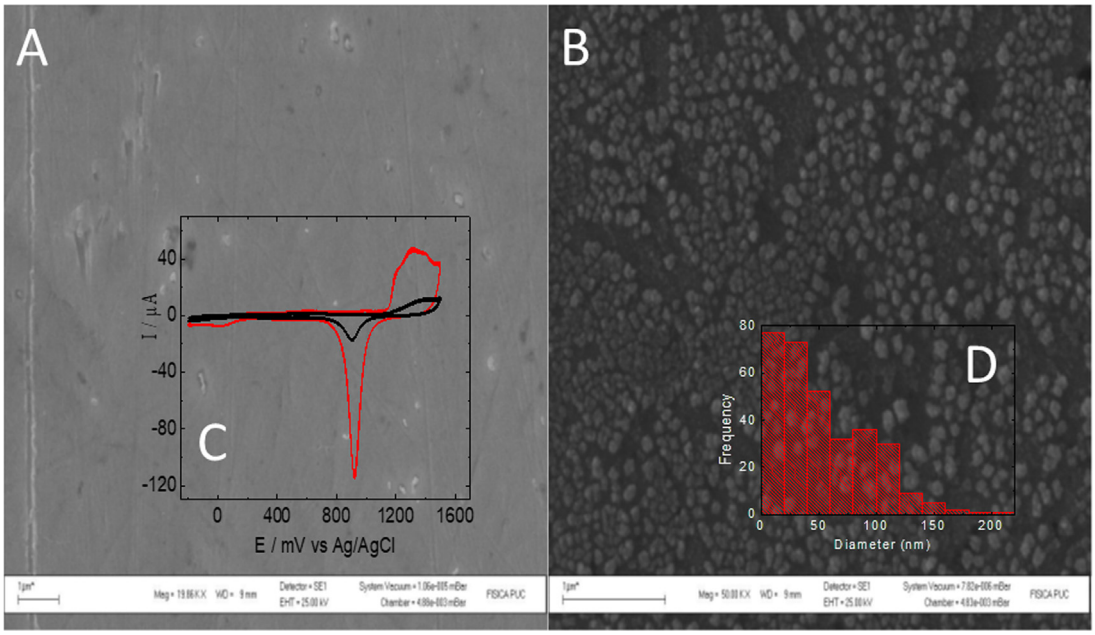

Fig. 1. SEM images of (A) planar gold electrode; (inset (C): Cyclic voltammograms of planar gold electrode and gold nanoparticles electrode in aqueous 0.5 mol L^{-1} H_2SO_4 solution. Scan rates were 50 mV s^{-1}) and (B) gold nanoparticles electrode obtained at a fixed potential of −0.2 V (vs. Ag/AgCl) for 330 s, at 80 °C and $2{\cdot}10^{-3}$ mol L^{-1} of $HAuCl_4$ in 0.1 mol L^{-1} KNO_3; (inset (D): Histogram showing the particle size distributions of gold nanoparticles.).

subsequently aliquoted at a dilution of 1:100 in PBS (pH 7.4). These aliquots were also stored at −20 °C and used separately (to prevent thawing and freezing) in each of the experiments.

For the reduction of thiol group in the hinge region of the antibody, 2-mercaptoethanol (2-ME) was used as a reducing agent. For this, intact antibody was dissolved at 20 µg mL^{-1} in a 0.1 M PBS (pH 6) containing 0.15 mol L^{-1} NaCl and 5.0 mmol L^{-1} EDTA. Then, 12 mg of 2-ME were added to 1.0 mL of this solution and incubated at 37 °C for 2 h , such that the 2-ME split the heavy chains of the antibody without separating its light chains. Subsequently, the above solution is transferred to a 1 mL plastic tube containing a dialysis membrane with a pore size of 3000 Da (Vivaspin500- 3000 Da Sartorius Vs0191), and centrifuged at 11.000 rpm for 30 min. The filtrate (which contains the molecules at a molecular weight of less than 3000 Da) is separated and discarded. To the supernatant is added 1 mL of the same buffer in which the antibody is dissolved and centrifuged again. This process is repeated 3 times to ensure that all molecules smaller than 3000 Da are separated from the solution to leave only the antibody and its fractions. Finally, 1 mL of 50% glycerol is added to the final solution of the half-antibody and stored at −20 °C for further electrophoresis analysis.

The electrophoresis analysis was carried out in SDS-PAGE 10% gels with the only difference being that the sample buffer was prepared without 2-ME in order to not affect the antibodies.

2.5. Adsorption of antibodies

An aliquot of 20 µL of the Ab and H-Ab solution was added over the nanostructured electrode and incubated for 2 h at 4 °C, then washed thoroughly with PBS pH 7.4 and milli-Q water. Finally, 1.0% BSA solution was added to block the non-specific reactive sites. Subsequently, the electrodes were cleaned and stored with PBS (pH = 7.4) solution for further electrochemical measurement.

2.6. Electrochemical measurements

Cyclic voltammetry (CV) and electrochemical impedance spectroscopy (EIS) were performed in a solution containing 1.0 mol L^{-1} $K_3[Fe(CN)_6]/K_4[Fe(CN)_6]$ in KCl 0.1 mol L^{-1} between 0 to + 0.6 V at a scan rate of 50 mV s^{-1} for CV. The EIS measurements were carried out over a frequency range of 100 kHz to 0.01 Hz and an applied potential of 0.23 V using a modulation voltage of 10 mV. These electrochemical experiments were carried out under the atmosphere of nitrogen.

2.7. CRH detection

Commercially lyophilized peptides (CRH and UCN I) were aliquoted and stored at −20 °C in milli-Q water at 1 mg mL^{-1}, and 20 µL of CRH of different concentrations were added on the surface for 2 h at 4ºC. Subsequently, the modified electrode was washed 3 times with PBS 0.1 mol L^{-1} at pH 7.4 and stored for further electrochemical measurements. In order to ensure specificity, electrodes were exposed to Urocortin I (peptide from the same family as CRH) and stored for further electrochemical measurements.

2.8. Sample analysis

Human serum samples were stored at − 20 ∘C. When used, the liquid was reconstituted in PBS for a final concentration of 20 µg mL^{-1} CRH by gentle stirring and mixing up to total dissolution. CRH detection was performed by applying the procedure described above, and the charge transfer resistance values measured by EIS were interpolated into the linear portion of the calibration plot obtained with CRH standard solutions.

3. Results and discussion

3.1. Characterization and optimization of the obtainment of AuNp

Fig. 1A and B show the SEM images of the unmodified bare gold electrode (Au), displaying a smooth structure and the modified gold nanoparticles electrode (Au/AuNp) obtained under optimal conditions, showing a rough surface and, in general, a uniform distribution of different sized groups of AuNp, respectively. Additionally, not all of the nanoparticles presented a spherical shape, as a considerable portion show an irregular shape.

Inset Fig. 1D displays a histogram with the size frequency of the

nanoparticles. The size of AuNp fluctuates between 20 and 200 nm, but with a larger proportion between 20 and 120 nm. Other research where AuNp is obtained at room temperature, but using similar electrochemical conditions for obtainment, show a nanoparticle sizes that ranges between 30 and 60 nm (Liu et al., 2005; Park et al., 2011). On the other hand, a cyclical voltammetry study was performed to estimate the roughness factor of Au and Au/AuNp (inset Fig. 1C). This considers the voltammetric responses obtained in H_2SO_4 0.5 mol L^{-1} in the absence of oxygen. The estimated roughness factor may be determined based on the peak reduction presented by the electrodes, considering the desorption charge (390 μC/cm^2) of gold oxide (Xiao et al., 2016). The determined area of Au and Au/AuNp was 0.069 ± 0.006 cm^2 and 0.728 ± 0.013 cm^2, respectively. Upon calculation of both roughness factors, the ratio of Au to Au/AuNp obtained was 1:10.5, which highly exceeds that reported by Park et al. (2011) of 1:1.17 and by Liu et al. (2005) of 1:1.29. The comparison of these results shows that the experimental conditions play a fundamental role in the electrochemical obtainment of AuNp affecting the roughness factor.

To optimize the obtainment of Au/AuNp, we evaluated the effect of three parameters in the electrodeposition of AuNp: applied potential, concentration of $HAuCl_4$ and temperature. For this, a voltammetric response study of each electrode was performed in the presence of the redox couple $Fe(CN)_6^{-3/-4}$ in KCl 0.1 mol L^{-1} in a window of potential from 0 to + 0.6 V. Fig. 2A shows the cyclical voltammetry of Au (curve a) and Au/AuNp obtained in optimal conditions (curve b). In both cases, a redox process at + 0.23 V was observed, which presents a diffusion-controlled behaviour, which has already been described by other authors (Liu et al., 2005). The maximum anodic currents obtained from both voltammetric profiles were determined, and the difference in current (ΔI/μA) was used to compare and obtain reproducible electrodes.

The obtainment of Au/AuNp was performed based on a dissolution $2{\cdot}10^{-3}$ mol·L^{-1} of $HAuCl_4$ in KNO_3 0.1 mol L^{-1} at different fixed potentials between −0.1 V and −0.5 V for 330 s and a constant temperature of 25 °C (data not shown). It was observed that the Au/AuNp obtained at −0.1 V presents the same response (ΔI/μA) as Au, indicating that there is no growth of AuNp. When applying fixed potentials between −0.2 V and −0.5 V the response of Au/AuNp (ΔI/μA) increased in comparison to Au, regardless of the fixed potential applied for obtaining AuNp. Based on these results, a potential of −0.2 V was chosen for application

Fig. 2B and C show the effect of the concentration of $HAuCl_4$ and temperature in the increased response (ΔI/μA) of the electrodes obtained. Both plots show an increased response (ΔI/μA) when increasing the temperature and concentration, but some conditions show greater standard deviations in the variations of current (ΔI/μA), therefore, to obtain reproducibility in the AuNp-modified electrodes, the following optimal conditions were selected: fixed potential of −0.2 V for 330 s, 80 °C and $2{\cdot}10^{-3}$ mol·L^{-1} of $HAuCl_4$.

3.2. Obtainment and characterization of the electrochemical immunosensor

Fig. 3 charts the electrochemical systems studied. At the top, the immobilization of the intact antibody (Ab) is shown, and at the bottom the immobilization of the half-antibody (H-Ab) on an Au/AuNp electrode. Then, both systems were incubated with a concentration of 20 μg mL^{-1} of CRH, and an electrochemical impedance study was performed in the presence of the redox couple $Fe(CN)_6^{-3/-4}$ in KCl 0.1 mol L^{-1}.

Fig. 4A shows the Nyquist diagrams obtained for the different phases for obtaining the electrochemical immunosensor with the Ab and its subsequent incubation in the CRH antigen. The Au/AuNp electrode shows a low charge transfer resistance (R_{CT}) due to its conduction characteristics. The first step was to directly incubate the Ab on the AuNp, and the impedance results show an increase in the R_{CT}. This increase indicates that the nanostructured surface was modified with the Ab, as described by Rezaei et al. (2011). The second step was to

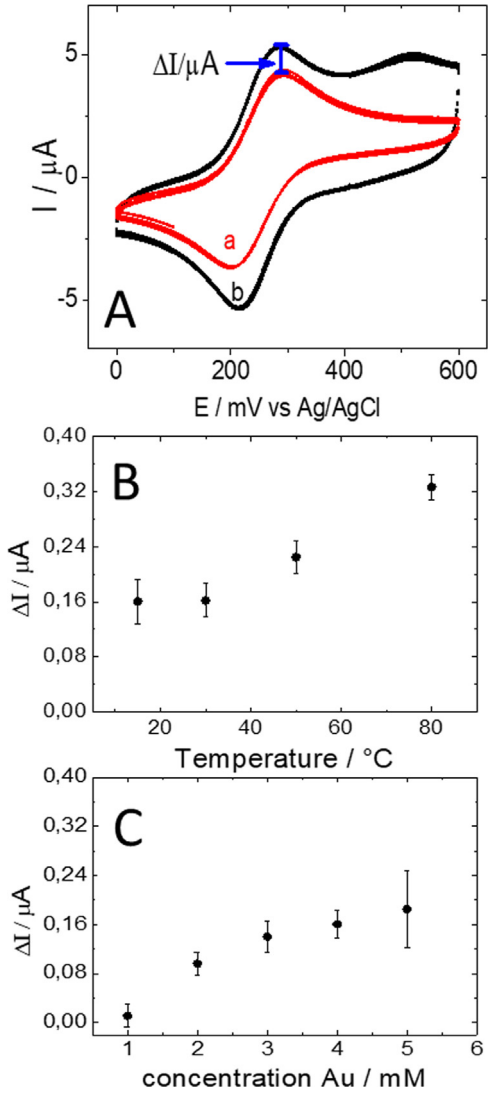

Fig. 2. (A) Cyclic voltammograms of 1.0 mol L^{-1} $K_3[Fe(CN)_6]/K_4[Fe(CN)_6]$ in KCl 0.1 mol L^{-1} between 0 to + 0.6 V. Scan rate were 50 mV s^{-1} on bare gold electrode (**curve a**) and gold nanoparticles electrode (**curve b**). The effect of the temperature (B) and concentration of $HAuCl_4$ (C) in the increased current response (ΔI/μA).

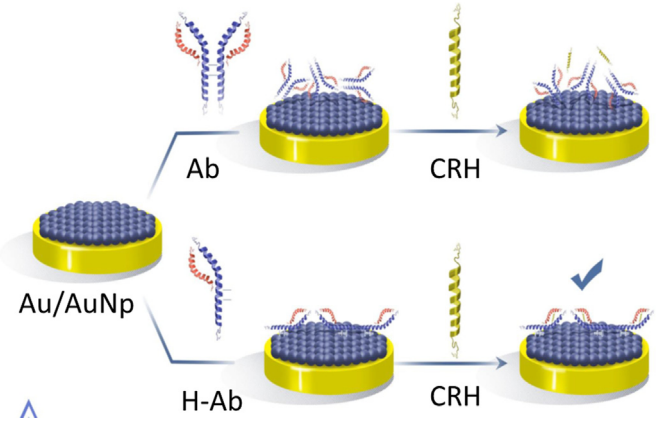

Fig. 3. Scheme of the oriented immobilization of intact antibody (top) and half antibody fragments (bottom) on Au/AuNp electrode, oriented immobilization of half antibody fragments via their own thiol groups conjugated to the AuNp by a single-step. Both electrodes were incubated in CRH, only obtaining response with Au/AuNp/H-Ab electrode.

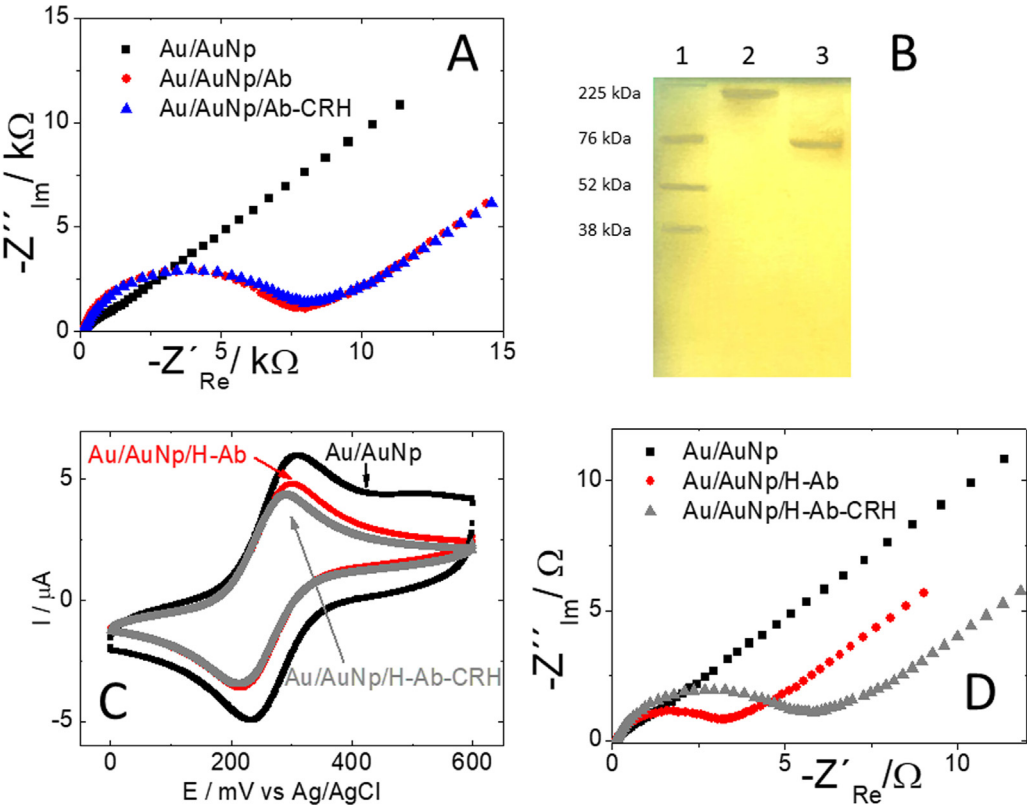

Fig. 4. (A) Nyquist diagrams of Au/AuNp electrode (**black squares**); Au/AuNp/Ab (**red circles**) and Au/AuNp/Ab-CRH (The concentration of CRH is 20 µg mL^{-1}) (**blue triangles**) in solution composition: 1.0 mol L^{-1} M $K_3[Fe(CN)_6]/K_4[Fe(CN)_6]$ in KCl 0.1 mol L^{-1}; (B) SDS–PAGE analysis (10% gel) protein molecular weight standards (line 1), purified intact antibodie (line 2) and half antibody obtained after reduction with 2-ME (line 3); (C) Cyclic voltammograms of: Au/AuNp (**black line**); Au/AuNp-H-Ab (**gray line**); Au/AuNp/H-Ab-CRH (**red line**) Scan rate: 50 mV s^{-1}; (D) Nyquist diagrams of Au/AuNp electrode (**black squares**); Au/AuNp/H-Ab (**red circles**) and Au/AuNp/H-Ab-CRH (The concentration of CRH is 20 µg mL^{-1}) (**gray triangles**) in solution composition: 1.0 mol L^{-1} $K_3[Fe(CN)_6]/K_4[Fe(CN)_6]$ in KCl 0.1 mol L^{-1}. EIS: 0.01 Hz and 100 kHz, 10 mV of amplitude and potential bias of 0.23 V. (For interpretation of the references to color in this figure legend, the reader is referred to the web version of this article.)

incubate the CRH antigen at different times on the Au/AuNp-Ab electrode, and then perform the electrochemical impedance, which showed the same behaviour in the absence and presence of the CRH antigen. This indicates that the Ab does not interact with the CRH antigen, and, therefore, there are no changes in the electrical properties of the electrode/dissolution interface. The performance of a bio / immunosensor depends on three critical factors: (i) its capacity to immobilize recognition elements (biological molecules) while maintaining their natural activity; (ii) the accessibility of the recognition element to the relevant antigen in dissolution; and (iii) low adsorption non-specific to the solid support. The physical-chemical properties of the surface or sensor play an important role in achieving the optimal immobilization of Ab and limiting non-specific adsorption (Sharma et al., 2016).

An alternative method for obtaining an electrochemical immunosensor response was to perform the fragmentation of Ab by its heavy chains, using 2- mercaptoethanol as a redactor agent, the reduction reaction of the thiol groups located in the two heavy chains does not affect the specific antibody binding sites (Makaraviciute and Ramanaviciene, 2013; Baniukevic et al., 2013, 2012). Fig. 4B displays the electrophoresis gel obtained, and track 1 shows the molecular weight standards (Rainbow Molecular weight Marker, GE Healthcare Life Science), while track 2 shows a single band corresponding to approximately ~200 kDa, this marker corresponds to the intact Ab. Track 3 only shows a band of around ~76 kDa, corresponding to the H-Ab, and indicates that the reduction of the antibody disulfide bridges produces fragmentation in two parts of the same mass, and these results are similar to those that have been reported (Hu et al., 2010; Makaraviciute et al., 2016). The H-Ab obtained remained stable and was stored in 50% of glycerol at −20 °C for its subsequent use in the development of the electrochemical impedimetric immunosensor.

Fig. 4C and D show the electrochemical study by VC and EIS in the different steps taken to obtain the electrochemical immunosensor with the H-Ab and its subsequent incubation in the CRH antigen. The VC and Nyquist diagrams show different electrochemical responses between the Au/AuNp, Au/AuNp/H-Ab and Au/AuNp/H-Ab-CRH electrodes. As can be seen in Fig. 4D, the Au/AuNp/H-Ab presents an increase in the R_{CT}, this change corroborates the adsorption of H-Ab on the AuNp. After the incubation of Au/AuNp/H-Ab in the presence of CRH, an increase in R_{CT} is seen once again, indicating the antigen-antibody interaction. Additionally, the specificity of Au/AuNp/H-Ab was evaluated by incubating 20 µg mL^{-1} of UCN I. Urocortin belongs to the family of Corticotropin-releasing factors, which also includes CHR. This assay produces no changes in the electrochemical impedance response (data not shown).

One of the advantages of H-Ab is the specific orientation of the antibody achieved by the interaction of free S-groups with AuNp. This quality has been studied by a number of authors (Crivianu-Gaita and Thompson, 2015; Karyakin et al., 2000; Sharma and Mutharasan, 2013; Shen et al., 2017; Wu et al., 2014), which use electrochemical techniques to show that treatment with 2-ME promotes a rupture of the thiol groups and, subsequently, a specific orientation of the antibody on the nanostructured surface.

In addition, this way of immobilization allows these systems to avoid the loss of their biological activity, since the immobilization of H-Ab occurs in a robust form, which allows the obtainment of a homogeneous and high density of the binding site for the CRH (Makaraviciute et al., 2016; Shen et al., 2017).

Also, this study shows that the rupture and orientation of the antibody on the nanostructured surface allows for an adequate detection of the CRH antigen. This is because the region where the thiol groups are located in the H-Ab, and which correspond to the bond sites with the AuNp, are different from the binding sites to CRH.

3.3. Quantitative detection of CRH

Immunodetection of CRH was based on the measurement of faradaic impedance in the presence of the redox couple $[Fe(CN)_6]^{3-/4-}$ in KCl 0.1 mol L^{-1}. The R_{CT} of the redox probe reflects the amount of CRH attached on the surface in a concentration-dependent manner. A typical impedance spectrum recorded for increasing concentrations of CRH on

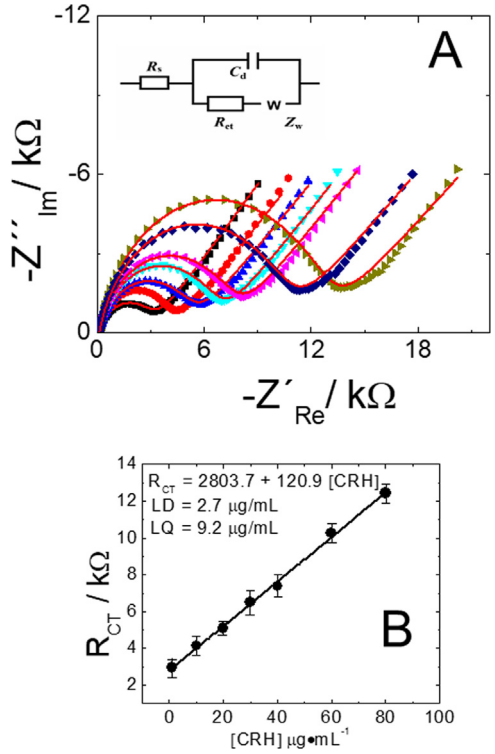

Fig. 5. (A) Nyquist diagrams of impedance spectra recorded with CRH immunosensors. The imaginary component of impedance ($-Z''/k\Omega$) is presented as a function of the real component ($Z'/k\Omega$). Impedance spectra were recorded in 1.0 mol L^{-1} $K_3Fe(CN)_6/K_4Fe(CN)_6$ in KCl 0.1 mol L^{-1} over the frequency range from 100 kHz to 0.01 Hz using a bias potential of 0.23 V vs. Ag/AgCl reference electrode. The amplitude of the alternating voltage was 10 mV. The spectra show data from functional immunosensors before and after CRH recognition. Sequential profiles are: (a) without any analyte (CRH), (b) with 10 µg mL^{-1} CRH; (c) 20 µg mL-1; (d) 30 µg mL^{-1}; (e) 40 µg mL^{-1}, (f) 60 µg mL^{-1}; (g) 80 µg mL^{-1}; (B) Calibration curves for CRH immunosensors. The R_{CT} (kΩ) is presented as a function of CRH concentration (µg mL^{-1}).

Au/AuNp/H-Ab is shown as Nyquist plots in Fig. 5A. A significant difference in the impedance spectrum upon the addition of increasing CRH concentrations can be observed. The changes in the electrochemical properties of the system were simulated using the Randles equivalent circuit model (inset Fig. 5A). The quality of the fitting to the equivalent circuit was evaluated by an acceptable error value of $\chi^2 < 0.001$ (Table 1S, supplementary material).

To obtain a calibration curve, R_{CT} was plotted against the CRH concentration. The linear range was between 10.0 and 80.0 µg mL^{-1} ($r^2 = 0.996$) (n = 3) with a slope value of 120.9 µg $mL^{-1} \cdot R_{TC}^{-1}$ (Fig. 5B). Limit of detection (LOD) and limit of quantification (LOQ), 2.7 µg mL^{-1} and 9.2 µg L^{-1}, respectively, were calculated using the following equations: LOD = 3 s/m, LOQ = 10 s/m, where s is the standard deviation of value of the R_{CT} as H-Ab is immobilized on the electrode surface (baseline of the blank, three measurements) and m is the slope of the calibration curve (Ramírez et al., 2016).

The interaction between the H-Ab and CRH is characterized by its affinity constant, K_a, defined by the equilibrium concentrations of the H-Ab–CRH complex. According to the Langmurian theory, association constant of the surface-immobilized antibody and its specific binding antigen is described as the variation of the relative impedance, $(R_{CT(i)} - R_{CT(0)}/R_{CT(0)}$, where $R_{CT(0)}$ is the value of the charge transfer resistance as H-Ab is immobilized on the electrode surface, and $R_{CT(i)}$ is the value of the charge transfer resistance after binding CRH to H-Ab (Rezaei et al., 2011). Therefore the slope of calibration curve (Fig. 1S supplementary material) can be used to calculate the association constant, Ka, where concentrations are in molar. CRH has an affinity constant of $1.96 \cdot 10^5$ M^{-1} toward half-polyclonal rat CRH antibody immobilized on the surface of the AuNp electrode.

The detection of CRH in serum samples was performed with a standard method of recovery percentage to check for the existence of interferences (Table 2S supplementary material), which indicates that there was no significant cross-reaction of the components of the serum with the immunosensor. The relative standard deviation (RSD) of the four measurements (n = 4) for the electrode in absence and presence of serum was 2.21% and 3.85%, suggesting that the precision and reproducibility of the immunosensor was good. Moreover, it has shown considerable repeatability and reproducibility data (Fig. 2S supplementary material), that confirms a promising alternative for the direct detection of CRH in biological fluids with minimum interferences. In order to test the stability, we stored the electrochemical immunosensor at 4 °C for nine days. After a storage period, the immunosensor still retained 89% of its initial charge transfer resistance (R_{CT}) response, indicating a satisfactory stability.

We have compared our experimental data with previously reported literature (Table 3S supplementary material). The electrochemical immunosensor proposed in this work presents a LOD of 2.7 µg mL^{-1} and the LOQ limits reported are around 0.5 µg mL^{-1} using liquid chromatography–Tandem mass spectrometry in placental tissue (Fahlbusch et al., 2013) and LOD of around 0.2 ng mL^{-1} in human blood. Therefore, at this time the device is being optimized by using an anti-CRH monoclonal half-antibody to increase sensitivity and to be used in blood (plasma and serum).

4. Conclusions

A simple Au/AuNp/H-Ab-based nanostructured platform for the electrochemical detection of CRH was developed. To obtain reproducibility in electrodes modified with AuNp, the following optimal conditions were chosen: fixed potential of −0.2 V for 330 s, 80 °C and 2 mM of $HAuCl_4$. The electrochemical immunosensor detected CRH within the concentration ranges of 10 µg mL^{-1} to 80 µg mL^{-1}, and an LOD of 2.7 µg mL^{-1}. The platform used for anti-CRH half-antibody immobilization presented good reproducibility and stability, hence providing a great start for the construction of a novel immunosensor for clinical diagnosis and other biosensor applications. Future experiments may focus on the use of monoclonal half-antibodies to increase sensitivity, the evaluation of interference and its use in the detection of CRH in real samples.

CRediT authorship contribution statement

B.G. Duran: Investigation, Methodology. **E. Castañeda:** Investigation, Methodology. **F. Armijo:** Investigation, Methodology.

Acknowledgements

This research was supported financially by Fondecyt (Chile) 1150228 and 3170784.

Declaration of interests

None.

Appendix A. Supporting information

Supplementary data associated with this article can be found in the online version at doi:10.1016/j.bios.2019.02.017.

References

Baniukevic, J., Ramanavicius, A., Ramanaviciene, A., 2012. Procedia Eng. 47, 837–840.
Baniukevic, J., Kirlyte, J., Ramanavicius, A., Ramanaviciene, A., 2013. Sens. Actuators B

189, 217–223.
Cook, C.J., 2001. J. Neurosci. Methods 110, 95–101.
Crivianu-Gaita, V., Thompson, M., 2015. Biosens. Bioelectron. 70, 167–180.
Dunlop, B.W., Wong, A., 2019. Prog. Neuropsychopharmacol. Biol. Psychiatry 89, 361–379.
Endsin, M.J., Michalec, O., Manzon, L.A., Lovejoy, D.A., Manzon, R.G., 2017. Gen. Comp. Endocrinol. 240, 162–173.
Fahlbusch, F.B., Ruebner, M., Rascher, W., Rauh, M., 2013. Steroids 78, 888–895.
Glynn, L.M., Schetter, C.D., Chicz-DeMet, A., Hobel, C.J., Sandman, C.A., 2007. Peptides 28, 1155–1161.
Hermanson, G.T., 2013. Bioconjugate Techniques, 3rd ed. Academic Press, Oxford.
Hu, C.-M.J., Kaushal, S., Cao, H.S.T., Aryal, S., Sartor, M., Esener, S., Bouvet, M., Zhang, L., 2010. Mol. Pharm. 7, 914–920.
Jazayeri, M.H., Amani, H., Pourfatollah, A.A., Pazoki-Toroudi, H., Sedighimoghaddam, B., 2016. Sens. Biosensing. Res. 9, 17–22.
Justino, C.I.L., Freitas, A.C., Pereira, R., Duarte, A.C., Rocha Santos, T.A.P., 2015. Trends Anal. Chem. 68, 2–17.
Karyakin, A.A., Presnova, G.V., Rubtsova, M.Y., Egorov, A.M., 2000. Anal. Chem. 72, 3805–3811.
Kaushik, A., Vasudev, A., Arya, S.K., Bhansali, S., 2013. Biosens. Bioelectron. 50, 35–41.
Khan, M.S., Vishakante, G.D., Siddaramaiah, H., 2013. Adv. Colloid Interface Sci. 199–200, 44–58.
Knoop, A., Thomas, A., Bidlingmaier, M., Delahaut, P., Schanzera, W., Thevis, M., 2017. Anal. Methods 9, 4304–4310.
Liu, G., Zhang, Y., Guo, W., 2004. Biosens. Bioelectron. 61, 547–553.
Liu, S.-F., Li, X.-H., Li, Y.-C., Li, Y.-F., Li, J.-R., Jiang, L., 2005. Electrochim. Acta 51, 427–431.
Makaraviciute, A., Ramanaviciene, A., 2013. Biosens. Bioelectron. 50, 460–471.
Makaraviciute, A., Jackson, C.D., Millner, P.A., Ramanaviciene, A., 2016. J. Immunol. Methods 429, 50–56.
Merali, Z., Khan, S., Michaud, D.S., Shippy, S.A., Anisman, H., 2004. Eur. J. Neurosci. 20, 229–239.
Moreno-Guzman, M., Eguılaz, M., Campuzano, S., Gonzalez-Cortes, A., Yañez-Sedeño, P., Pingarron, J.M., 2010. Analyst 135, 1926–1933.
Moreno-Guzman, M., Gonzalez-Cortes, A., Yañez-Sedeño, P., Pingarron, J.M., 2012a. Electroanalysis 24, 1100–1108.
Moreno-Guzmán, M., Ojeda, I., Villalonga, R., González-Cortés, A., Yañez-Sedeño, P., Pingarrón, J.M., 2012b. Biosen. Bioelectron. 35, 82–86.
Pang, X., Cui, C., Su, M., Wang, Y., Wei, Q., Tan, W., 2018. Nano Energy 46, 101–109.
Park, B.-W., Yoon, D.-Y., Kim, D.-S., 2011. J. Electroanal. Chem. 661, 329–335.
Ramírez, C., del Valle, M.A., Isaacs, M., Armijo, F., 2016. Electrochim. Acta 199, 227–233.
Ren, X., Zhang, T., Wu, D., Yan, T., Pang, X., Du, B., Lou, W., Wei, Q., 2017a. Biosens. Bioelectron. 94, 694–700.
Ren, X., Yan, J., Wu, D., Wei, Q., Wan, Y., 2017b. ACS Sens. 2, 1267–1271.
Ren, X., Ma, H., Zhang, T., Zhang, Y., Yan, T., Du, B., Wei, Q., 2017c. ACS Appl. Mater. Interfaces 9, 35260–35267.
Ren, X., Lu, P., Feng, R., Zhang, T., Zhang, Y., Wu, D., Wei, Q., 2018. Talanta 188, 593–599.
Rezaei, B., Majidi, N., Rahmani, H., Khayamian, T., 2011. Biosens. Bioelectron. 26, 2130–2134.
Ricci, F., Adornetto, G., Palleschi, G., 2012. Electrochim. Acta 84, 74–83.
Rusling, J.F., Sotzing, G., Papadimitrakopoulosa, F., 2009. Bioelectrochemistry 76, 189–194.
Saha, K., Agasti, S.S., Kim, Ch, Li, X., Rotello, V.M., 2012. Chem. Rev. 112, 2739–2779.
Saldan, I., Dobrovetska, O., Sus, L., Makota, O., Pereviznyk, O., Kuntyi, O., Reshetnyak, O., 2018. J. Solid State Electrochem. 22, 637–656.
Sandman, C.A., Glynn, L., Schetter, C.D., Wadhwa, P., Garite, T., Chicz-DeMet, A., Hobel, C., 2006. Peptides 27, 1457–1463.
Santibañez, M., Gysling, K., Forray, M.I., 2005. J. Neurosci. Res. 81, 140–152.
Santibañez, M., Gysling, K., Forray, M.I., 2006. J. Neurosci. Res. 84, 1270–1281.
Sharma, H., Mutharasan, R., 2013. Anal. Chem. 85, 2472–2477.
Sharma, S., Byrne, H., O'Kennedy, R.J., 2016. Essays Biochem. 60, 9–18.
Shen, M., Rusling, J.F., Dixit, C.K., 2017. Methods 116, 95–111.
Strong, E.F., Kleinman, K.P., Gillman, M.W., Clark, I., Emanuel, R.L., Majzoub, J.A., Rich-Edwards, J.W., 2006. Paediatr. Perinat. Epidemiol. 20, 67–71.
Wu, S., Liu, H., Liang, X.M., Wu, X., Wang, B., Zhang, Q., 2014. Anal. Chem. 86, 4271–4277.
Xiao, X., Si, P., Magner, E., 2016. Bioelectrochemistry 109, 117–126.
Yamaguchi, M., Matsuda, Y., Sasaki, S., Sasaki, M., Kadoma, Y., Imai, Y., Niwa, D., Shetty, V., 2013. Biosens. Bioelectron. 41, 186–191.
Yang, L., Zhu, W., Ren, X., Khan, M.S., Zhang, Y., Du, B., Wei, Q., 2017a. Biosens. Bioelectron. 91, 842–848.
Yang, L., Li, Y., Zhang, Y., Fan, D., Pang, X., Wei, Q., Du, B., 2017b. ACS Appl. Mater. Interfaces 9, 37637–37644.
Zhao, P., Li, N., Astruc, D., 2013. Coord. Chem. Rev. 257, 638–665.
Zhou, J.C., Chuang, M.H., Lan, E.H., Dunn, B., Gillmanb, P.L., Smith, S.M., 2004. J. Mater. Chem. 14, 2311–2316.